Magnetic Properties of the Fe2SiO4–Fe3O4 Spinel Solid Solutions

Article *in* Physics and Chemistry of Minerals · March 2001

DOI: 10.1007/s002690000135

CITATIONS
23

READS
238

2 authors, including:

Takamitsu Yamanaka
Carnegie Institution for Science
322 PUBLICATIONS **5,434** CITATIONS

SEE PROFILE

Phys Chem Minerals (2001) 28: 102–109

ORIGINAL PAPER

T. Yamanaka · M. Okita

Magnetic properties of the Fe_2SiO_4-Fe_3O_4 spinel solid solutions

Received: 20 April 2000 / Accepted: 11 September 2000

Abstract Magnetic measurement of $Fe_{3-x}Si_xO_4$ spinel solid solutions indicates that their Curie temperatures decrease gradually, but not linearly, from 851 to 12 K with increasing content of nonmagnetic ions Si^{4+}. Magnetic hysteresis becomes more noticeable in solid solutions having a larger content of Fe_2SiO_4. Saturation magnetizations of $Fe_{3-x}Si_xO_4$ samples increase up to $x = 0.357$ and they are easily saturated in the field of $H = 0.1$ T. However, magnetization of the sample of $x = 0.794$ does not approach saturation even at high field of $H = 7.0$ T and has a large coercive force. The Si^{4+} disordered distribution is confirmed to be $^{tetr}[Fe^{3+}_{1-x+xt}Si^{4+}_{x(1-t)}]$ $^{octa}[Fe^{2+}_{1+x}Fe^{3+}_{1-x-xt}Si^{4+}_{xt}]$ O_4 by the spin moment, which is consistent with site occupancy obtained from X-ray crystal structure refinement. Their molecular magnetizations would be expressed as $M_B = \{4(1+x) + 10xt\}\mu_B$ as functions of composition parameter x and Si^{4+} ordering parameter t of the solid solution. The sample of $x = 0.794$ is antiferromagnetic below the Néel temperature, mainly due to the octahedral cation interaction M_O–M_O, while both M_T–M_O and M_O–M_O interactions induce a ferrimagnetic property. Concerning magnetic spin configuration, in the case of $x > 0.42$, the lowest dε level becomes a singlet, resulting in no orbital angular momentum.

Key words $Fe_{3-x}Si_xO_4$ spinel solid solution · Saturation magnetization · Magnetic hysteresis · Bohr magneton · Curie temperature

Introduction

Various magnetic minerals exist widely in the Earth's crust and mantle. The incorporation of Fe^{3+} into oxide minerals and silicate spinel has received much attention due to the implication of redox reaction in the upper mantle and transition zone (O'Neill et al. 1993). Since magnetite is one of the most important magnetic materials for not only geophysical but also material sciences, a number of informative observations about their physical properties have been reported. Magnetite has various solid solutions with other spinel phases. A great number of ferrites $M^{2+}Fe_2O_4$ have been investigated for industrial usage. Among these systems, the solid solutions with silicate spinels such as the systems Mg_2SiO_4-Fe_3O_4 and Fe_2SiO_4-Fe_3O_4 are significant systems to elucidate the geoelectromagnetic phenomena induced from the Earth's constituents, because $(Mg, Fe)_2SiO_4$ spinel is considered to be a dominant phase in the lower part of the transition zone (Irifune and Ringwood 1987). Magnetite and γ-Fe_2SiO_4 have also been investigated in order to comprehend the oxidation potential in the mantle from the viewpoint of the charge transfer and cation disorder under high-pressure conditions (Mao et al. 1974; Pasternak et al. 1994; Fei et al. 1999) and at high temperature (Yamanaka 1986).

A spinelloid phase was first found in the system Fe_3O_4-Fe_2SiO_4 by Canil et al. (1990) and further phase relations between 7 and 9 GPa were reported by O'Neill and Canil (1992). Recently, we clarified the phase diagram of the pseudobinary system under high pressure (Ohtaka et al. 1997). Woodland and Angel (1998) reinvestigated the spinelloid phase region. The crystal structures of three spinelloids, phase II, phase III, and phase V, have been refined by Ross et al. (1992) and Woodland and Angel (1998). These structures are topologically analogous to nickel-aluminosilicate spinelloids (Ma 1974; Horioka et al. 1981; Akaogi et al. 1982).

Numerous papers have been reported about the electric conductivity and magnetic property of both end members of the solid solution in the system, Fe_3O_4 and Fe_2SiO_4. These properties are dependent on the cation distribution in the spinel structure. Verwey (1939) first proposed the structure transition by freezing the electron

T. Yamanaka · M. Okita
Department of Earth and Space Science
Graduate School of Science,
Osaka University, 1-1 Machikaneyama Toyonaka,
Osaka 560-0043, Japan
e-mail: 61400@center.osaka-u.ac.jp
Fax/Tel.: 081-6-6850-5793

hopping at the octahedral site of magnetite at low temperatures. Magnetic studies of the magnetite-spinel solid solutions in the systems, Fe_3O_4-$MgAl_2O_4$ (Harrison and Putnis 1995) and Fe_3O_4-$ZnFe_2O_4$ (Krupicka and Novàk 1987) were reported.

It was known that magnetite Fe_3O_4 has an inverse spinel structure of $^{tetr}(Fe^{3+})^{octa}[Fe^{2+}Fe^{3+}]O_4$, having a ferrimagnetic property with the Curie temperature of 851 K. On the other hand, γ-Fe_2SiO_4 has a normal spinel structure $^{tetr}(Si^{4+})^{octa}[Fe^{2+}Fe^{2+}]O_4$ and is characterized as paramagnetic above the Néel point of 12 K and antiferromagnetic below this temperature (Suito et al. 1984). Throughout this paper parentheses and brackets represent the tetrahedral and octahedral site, respectively.

Single-crystal structure refinements of the $Fe_{3-x}Si_xO_4$ spinel solid solutions with $x = 0.0, 0.090, 0.288, 0.750$, and 1.0 were previously undertaken of X-ray diffraction study (Yamanaka et al. 1998). It was clarified that not less than 20% of total silicon occupies the octahedral sites; Si^{4+} substitutes for Fe^{3+} in the octahedral site and occupies 3% of the octahedral cations. The spinel solid solution can be expressed by the following cation distribution, using the compositional parameter x and the disorder parameter t:

$$^{tetr}[Fe^{3+}_{1-x+xt}Si^{4+}_{x(1-t)}]^{octa}[Fe^{2+}_{1+x}Fe^{3+}_{1-x-xt}Si^{4+}_{xt}]O_4 \ ,$$

where cations in parentheses and brackets indicate tetrahedral and octahedral cations, M_T and M_O, respectively.

Physical properties of the $Fe_{3-x}Si_xO_4$ spinel solid solutions, except for the two end members, have never been studied as a function of composition. We investigated the electric conductivity of this solid solution series. Activation energy of electron hopping and Verwey transition temperature as a function of Si substitution in $Fe_{3-x}Si_xO_4$ have been clarified and these results are reported in another paper (Yamanaka et al. 2001).

In this paper saturation magnetization and Curie temperature are discussed as a function of x of $Fe_{3-x}Si_xO_4$ from the viewpoint of their cation distribution, tetrahedral cation (M_T) and octahedral cation (M_O), and lattice deformation.

Experiment

Samples used in the present magnetic measurement were synthesized under high-pressure conditions over 6 GPa. The sample preparation methods are presented in Table 1. The method using a multianvil apparatus was described in another paper (Yamanaka et al. 2001).

Magnetic susceptibility was measured by a super quantum interference detector (SQUID) and a vibrating sample magnetometer (VSM). The measurement of magnetization was carried out by VSM in the fixed magnetic field of 1.0 T at a temperature range from 293 to 873 K. The Curie temperature (T_C) was determined from the measurement. Temperature was measured by a thermocouple with an accuracy of ± 0.1 K. The saturation magnetization was measured in the variable magnetic field up to 7 T at several fixed temperatures from 1.8 to 300 K by SQUID. Magnetization was measured as a function of applied magnetic field with a rate of 20 mT s^{-1}. The accuracy of magnetization measurement is less than 10^{-8} Am^2. The SQUID measurement has an accuracy of ± 0.1 emu. Samples with a mass of $60 \sim 90$ mg were weighed within an accuracy of ± 0.1 mg.

Result

Nonstoichiometry

The main purpose of the present experiment focuses on the magnetic properties of the Fe_3O_4-Fe_2SiO_4 spinel solid solutions. It was known that magnetite has a large range of cation-deficient nonstoichiometry (Darken and Gurry 1945; Kronmuller and Walz 1980), which is dependent on the oxygen potential. Thus at the beginning of the present experiment, nonstoichiometry of magnetite was examined by saturation magnetization.

From the Verwey transition temperature (T_v) of nonstoichiometric magnetite (Aragon et al. 1985), the magnetite samples synthesized at high temperatures under ambient pressure showed $\delta = 0.005 \sim 0.02$ in $Fe_{3-\delta}O_4$. To examine the magnetic property dependence of nonstoichiometry, two samples of $Fe_{3-\delta}O_4$ were prepared at 1300 °C under $P_{O_2} = 10^{-4}$ and 10^{-8} at ambient pressure, and a highly stoichiometric sample of Fe_3O_4 was also prepared at 6 GPa and 1200 °C using a graphite heater. δ-Values of three samples presented in Table 2 were estimated from the observed T_v by electric

Table 1 Synthesis conditions of $Fe_{3-x}SiO_4$ spinel solid solutions

Mixing ratio[a] Mt:Fa	Pressure (GPa)	Temperature (°C)	Duration (h)	x[b] of $Fe_{3-x}Si_xO_4$	Recovered[c] phase
10:0	6.0	1200	5.0	1.00	Spinel
9:1	9.5	1150	4.0	0.091	Spinel
8:2	8.5	1200	1.5	0.199	Spinel
8:2	9.5	1175	12.0	0.266	Spinel
7:3	9.5	1155	12.0	0.288	Spinel
6:4	9.5	–	12.0	0.357	Spinel
2:8	10.0	1215	5.0	0.794	Spinel
0:10	8.0	1150	5.5	0.0	Spinel

[a] Mt = Fe_3O_4, Fa = Fe_2SiO_4
[b] x was determined with EPMA
[c] Phase identification of the recovered samples was made by X-ray powder diffraction

Table 2 Saturation magnetization of $Fe_{3-\delta}O_4$ nonstoichiometric magnetite

Sample	M_s (emu g^{-1})	M_s (μ_B)	T_v (K)	δ[a]	Synthesis condition
1	91.0	3.77	102.2	0.11	1 atm 1300 °C $P_{O_2} = 10^{-4}$
2	96.2	3.98	107.2	0.011	1 atm 1300 °C $P_{O_2} = 10^{-8}$
3	101.0	4.18	124.0	0.0	6 GPa 1200 °C

[a] δ represents the nonstoichiometry in $Fe_{3-\delta}O_4$

conductivity measurement (Yamanaka et al. 2001) referring to Aragon et al. (1985). The magnetite sample synthesized at high pressures was confirmed to be stoichiometric. Hence, all samples of $Fe_{3-x}Si_xO_4$ were prepared under high pressure using the graphite heater, and they could be regarded as stoichiometric compounds.

Magnetic hysteresis

The magnetization curve of samples of $x = 0.0$, 0.090, 0.199, 0.288, and 0.357 of $Fe_{3-x}Si_xO_4$ was observed under a magnetic field of up to $H = 1.0$ T. For the sample of $x = 0.794$, the observation was carried out up to $H = 7.0$ T. Hysteresis loops for all samples were measured at 1.8 and 300 K.

We found from electric conductivity measurements that the Verwey transition temperatures (T_v) of the solid solutions decrease from 124 K of $x = 0.0$ to 102.2 K of $x = 0.288$. All samples below T_v have a noncubic spinel structure due to charge order, which results from freezing the electron hopping. Above T_v the samples are cubic spinel. The electric conductivity measurement is reported in another paper (Yamanaka et al. 2001).

Magnetic hysteresis of four samples, $x = 0.0, 0.357$, and 0.794 at 1.8 K are presented in Fig. 1a and b, respectively, by magnetization per unit mass (emu g^{-1}). Magnetization (M) of all samples except $x = 0.794$ is easily saturated in the field of $H = 1.0$ T. However, the hysteresis of $x = 0.794$ shows the characteristics of metamagnetism, which is often found in the magnetic transition between antiferromagnetic and ferromagnetic. Magnetization linearly increases with H in a low field region and changes abruptly over $H = 2$ T. It cannot approach the apparent saturation even at a field as high as $H = 7.0$ T, and a noticeably large coercive force of about 5 kOe was observed at $M = 0$. The sample also has a large residual magnetization of 50 emu g^{-1} at $H = 0$. Fe_3O_4-rich samples have small coercivities and remanence.

With increasing Si^{4+} substitution in $Fe_{3-x}Si_xO_4$ with $x > 0.4$, the saturation magnetization (M_s) requires a larger external field and dM/dH becomes smaller. More substitution toward Fe_2SiO_4 involves a disordered distribution of nonmagnetic Si^{4+} ions in these samples and generates lower magnetic domains around the magnetic ions. Magnetic spins of the solid solutions with $x > 0.4$ are not perfectly parallel in these local lattices. Under sufficiently high fields over 2 T, magnetic spins are ordered in parallel fashion. In the case of $x = 0.794$, hysteresis indicates antiferromagnetic characteristics, as mentioned before. Then M_O–M_O interaction becomes dominant. This may imply that a large magnetic anisotropy is similar to the saturation magnetization of Fe_3O_4-$MgAl_2O_4$ solid solution (Harrison and Putnis 1995).

Saturation magnetization

The saturation magnetizations (M_s) of solid solutions $x = 0.0$, 0.090, 0.266, and 0.357 at $H = 1.0$ T and $x = 0.794$ at $H = 5.0$ T are presented as a function of temperature in Fig. 2. There is no obvious change in M_s at T_v. Thus, the lattice deformation due to the Verwey transition brings little change in spin and orbital angular moment in both structures at above and below T_v. The sample of $x = 0.794$ shows no real saturation magnetization even at the 7-T field. Accordingly, the apparent saturation value is determined by assuming a linear extension of the M–H curve in the ferromagnetic region (Morrish 1965). The M_s's of samples shows a continuous increase with x up to $x = 0.357$. The variation of M_s is a general Q-type ferromagnetic character defined by Néel definition, but as seen from Fig. 2, the sample of $x = 0.794$ shows a slighlty positive curve above $H = 2$ T. This feature indicates that the sample belongs to P-type ferromagnetic material. This difference in the magnetization type is caused by the spontaneous magnetization related to magnetic spin angular momentum and orbital angular momentum.

In Fe_3O_4-rich samples, the magnetizations are mainly induced from magnetic spin interaction between the nearest irons, M_T–M_O and M_O–M_O. However, when the occupancy of Si^{4+} exceeds that of Fe^{3+} at the tetrahedral site of sample such as $x = 0.794$, M_O–M_O interactions become dominant. The site occupancies of magnetic ions at the tetrahedral and octahedral sites define the saturation magnetization and thermal variation of the magnetization (Fig. 2).

On the assumption that magnetic moment is composed of only spin angular momentum without orbital angular momentum, magnetic cation distribution reflects the saturation magnetization of the solid solutions. If the Si^{4+} ion preferentially occupies the tetrahedral site from ion size effect, the substitution for Fe^{3+} in the tetrahedral site can be represented by charge normalization:

$$^{tetr}Fe^{3+} + {}^{oct}Fe^{3+} = {}^{tetr}Si^{4+} + {}^{oct}Fe^{2+} \quad . \tag{1}$$

Assuming the antiparallel magnetic spin in the tetrahedral and octahedral sites in the spinel lattice, the following magnetic spin configuration can be estimated in the ferrimagnetic region:

$$\underset{\rightarrow}{(Fe^{3+}_{1-x}}, \underset{5(1-x)\mu_B}{Si^{4+}_x})[\ \underset{\leftarrow}{Fe^{2+}_{1+x}}\ ,\ \underset{4(1+x)\mu_B}{\ } \underset{\leftarrow}{Fe^{3+}_{1-x}}\ \underset{5(1-x)\mu_B}{\ }]O_4 \tag{2}$$

M_B would be expressed as $4(1+x)\mu_B$ as a function of composition x of the solid solution. From the saturation

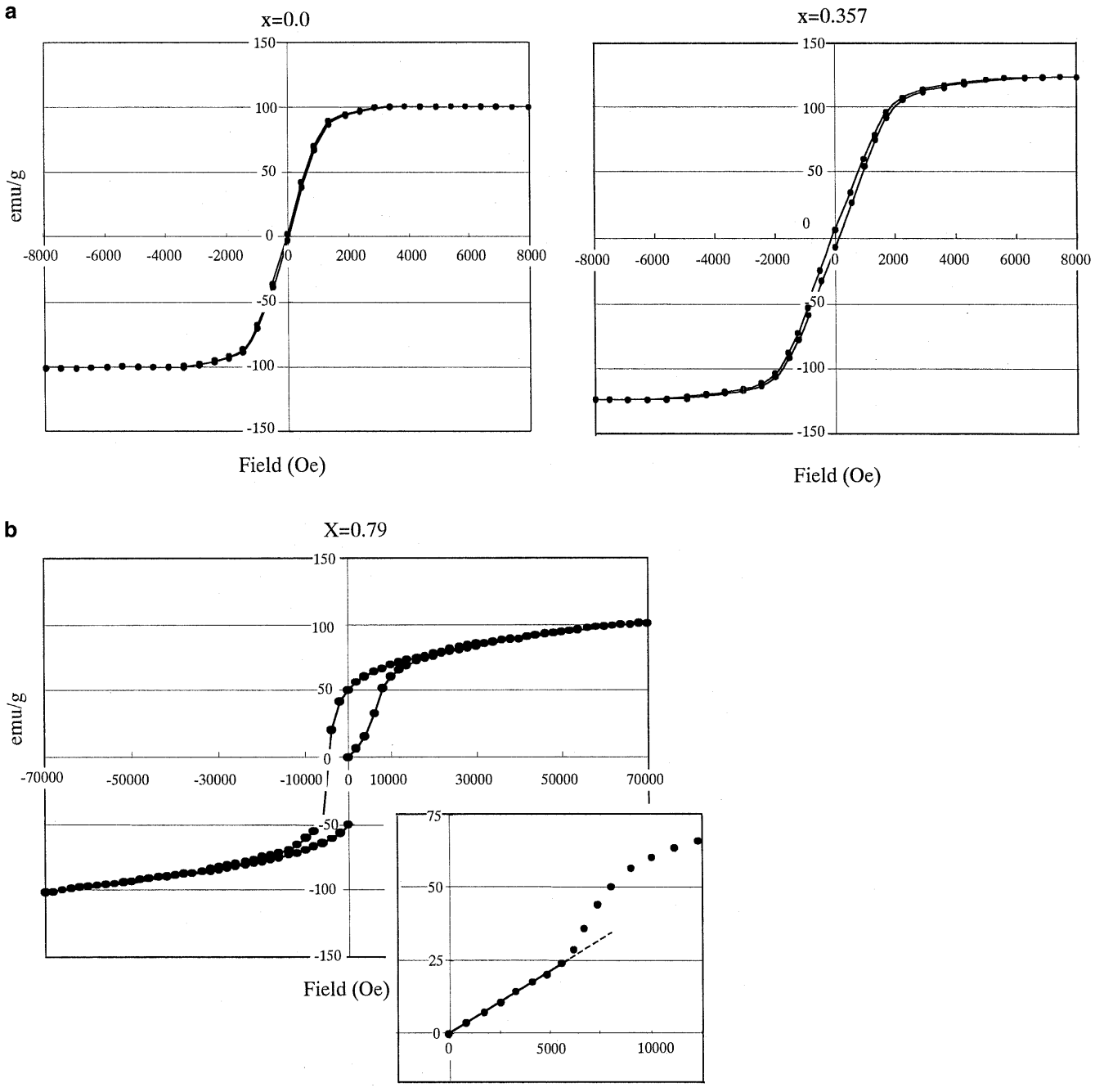

Fig. 1a, b Magnetic hysteresis of $x = 0.00$ and 0.357 of $Fe_{3-x}Si_xO_4$ spinel solid solutions observed under 1.0 T at 1.8 K (**a**) and that of $x = 0.794$ under 5.0 T at 1.8 K (**b**). The latter sample is an antiferromagnetic compound which is revealed by metamagnetism

magnetization, M_s, taken at 1.0 T and 20 K, Bohr magneton is calculated for the unit of $\mu_B(1\mu_B = 9.274 \times 10^{-24} J\,T^{-1} = 1.1653 \times 10^{-29}\,Wb\,m)$. The Bohr magneton changes with composition and then $M_B[= 4(1 + x)\,\mu_B]$ is led for the case of a constant J_{AB} in $M_s = gM_B J_{AB}$. When $x < 0.375$, the observed value is a little larger than the above M_B. This is partly because the Si^{4+} disordered distribution, which is shown in Eq. (5), ideally makes $M_B = [4(1 + x) + 10xt]\mu_B$. Those values of $Fe_{1-x}Zn_xO_4$ solid solutions between Fe_3O_4 and $ZnFe_2O_4$ are also plotted in Fig. 3. Magnetite ($x = 0.0$) shows $M_B = 4.2\mu_B$, which is a little greater than the ideal value of $4\mu_B$. The observed Néel point $T_N = 12$ K of γ-Fe_2SiO_4 accords well with Suito et al. (1984).

Curie temperature

The magnetic moment between A and B cations is given by the magnetic spin moments due to the A–B interaction between nearest-neighbor cations and those between second-neighbor A–A and B–B interactions. In the spinel structure M_T–M_O and M_O–M_O correspond to these interactions.

The following equation, based on the simple molecular field approximation (Hartree approximation), can be used to derive the Curie temperature:

$$T_c = \frac{W_{AB}}{2}\left[\alpha C_A + \beta C_B + \sqrt{4C_A C_B + (\alpha C_A - \beta C_B)^2}\right] , \quad (3)$$

where W_{AB} is the molecular field coefficient, and αW_{AB} and βW_{AB} are those of the A–A and B–B interaction, respectively. C_A and C_B are the Curie constants of A and B. As α and β are generally very small, W_{AB} is a dominant parameter; but W_{AB} is given by the internal magnetic field on each site and expressed by:

$$W_{AB} = \frac{2Z_{AB}|J_{AB}|}{N_B g^2 \mu_B^2} , \quad (4)$$

where Z_{AB} is the site occupancy of magnetic ion at the tetrahedral and octahedral site, g is the Lande factor, J_{AB} indicates the exchange coefficient of A–B interaction, and μ_B is the Bohr magneton unit.

According to Eqs. (3) and (4), the Curie temperature (T_c) linearly decreases with increasing content of nonmagnetic ions Si^{4+}. The variation of (T_c) is presented as a function of x of $Fe_{3-x}Si_xO_4$ in Fig. 4 and Table 3. Those of two other ferrites, $Fe_2Co_{1-x}Zn_xO_4$ and $Fe_2Mn_{1-x}ZnO_4$, are also plotted in the figure. All three compounds show the same trend of T_c with their composition. With increasing concentration of the nonmagnetic cation Si in the tetrahedral site of the silicate spinel structure, the Curie temperature is decreased. Compared with these two ferrites, the Curie temperature of $Fe_{3-x}Si_xO_4$ solid solution is slowly lowered with x. This is probably because the reduction of the A–B

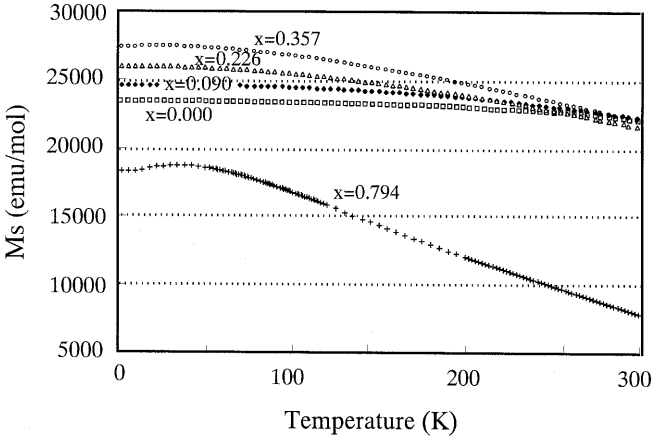

Fig. 2 Thermal change of the saturation magnetization of $Fe_{3-x}Si_xO_4$ spinel solid solutions. The saturation magnetization M_s of the solid solutions is plotted at elevated temperature. Those of $x = 0.0$, 0.090, 0.226, and 0.357 are observed at $H = 1.0$ T. In the case of $x = 0.794$, however, those data at $H = 5.0$ T are plotted, which is not a real saturation magnetization but the maximum value

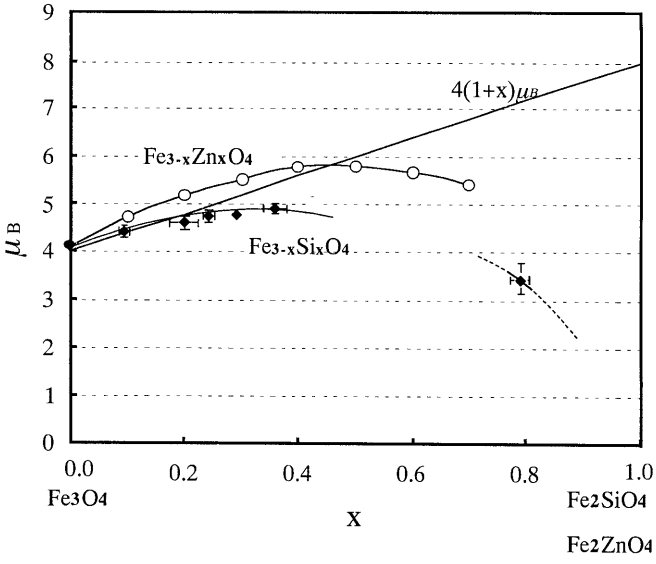

Fig. 3 Variation of the Bohr magneton with x of $Fe_{3-x}Si_xO_4$ spinel solid solutions. The variation of Bohr magneton is calculated from the molecular magnetization observed at 20 K. The *broken line* indicating $M = 4(1 + x)\mu_B$ shows the case of a constant J_{AB}. The Bohr magneton of $Fe_{3-x}Zn_xO_4$ spinel solid solutions is plotted for comparison

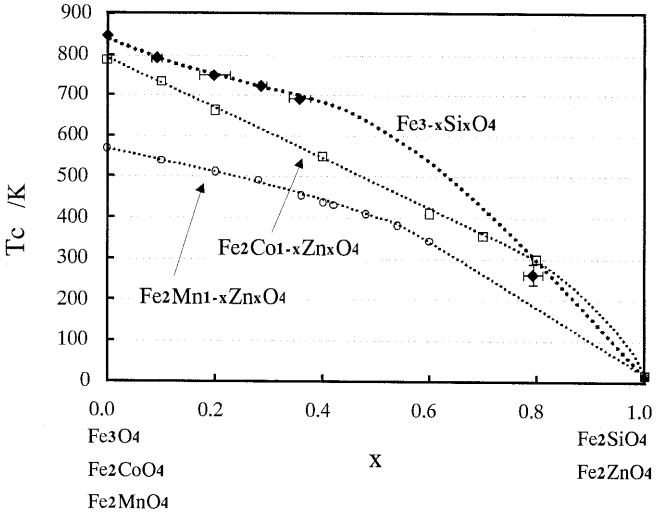

Fig. 4 Variation of Curie temperature T_c with x of $Fe_{3-x}Si_xO_4$ spinel solid solutions. Curie temperature of samples $x = 0.0$, 0.090, 0.199, 0.288, 0.357 were observed at the fixed field of 0.1 T using VSM (293 ~ 900 K) and SQID (4 ~ 300 K). That of $x = 0.794$ was at 5.0 T. Curie temperatures of $Fe_2Co_{1-x}Zn_xO_4$ and $Fe_2Mn_{1-x}Zn_xO_4$ are also plotted

Table 3 Curie temperature of $Fe_{3-x}Si_xO_4$ spinel solid solutions

x of $Fe_{3-x}Si_xO_4$	T_c (K)	Magnetism
0.000	851	Ferrimagnetic
0.090	790	Ferrimagnetic
0.199	749	Ferrimagnetic
0.288	723	Ferrimagnetic
0.357	691	Ferrimagnetic
0.794	260	Antiferromagnetic
1.000	12	Antiferromagnetic

interaction J_{AB} in Eq. (4) of $Fe_{3-x}Si_xO_4$ is a strong constraint.

Cation distribution

Saturation magnetization can be used to determine the cation distribution and order parameter of the magnetic ions in two-sites. The order parameter in hematite-ilmenite (Fe_2O_3-$FeTiO_3$) solid solution was determined from the magnetic moment (Brown et al. 1993).

Site occupancies of $Fe_{3-x}Si_xO_4$ were previously determined by X-ray structure refinement (Yamanaka et al. 1998). The cation distribution does not follow the simple substitution of Eq. (1) based on the Si^{4+} substitution only at the tetrahedral site. Assuming that all samples are stoichiometric, the cation distribution of $Fe_{3-x}Si_xO_4$ determined from the observed magnetization suggests the following equation instead of Eq. (1):

$$^{\text{tetr}}\left[Fe^{3+}_{1-x+xt}Si^{4+}_{x(1-t)}\right]^{\text{octa}}\left[Fe^{2+}_{1+x}Fe^{3+}_{1-x-xt}Si^{4+}_{xt}\right]O_4 \quad . \qquad (5)$$

The estimated cation distributions in the range of $x < 0.357$ are shown in Table 4. These distributions are based on Fe^{2+} preference to the octahedral site from the crystal field effect. The estimated distributions are consistent with the site occupancies from X-ray single-crystal analysis, as seen from Fig. 5. The present results of the site occupancy ratio (t) indicate the substitution of Si^{4+} into the octahedral site as a function of total Si^{4+}. The magnetite-rich part of $Fe_{3-x}Si_xO_4$ gradually increases the disorder and the value of t has a maximum at about $x = 0.375$. Then the disorder decreases toward the end member Fe_2SiO_4.

Marumo et al. (1974, 1977) examined possible disorder of Si^{4+} in both tetrahedral and octahedral sites of silicate spinels, Fe_2SiO_4, Co_2SiO_4, and Ni_2SiO_4, and they observed a small degree of cation disorder in Fe_2SiO_4 spinel ($x = 1.0$, $t = 0.023 \pm 0.01$). These studies prove that Fe^{2+} is preferentially located in the octahedral site, but a small amount of Fe^{2+} occupies the tetrahedral site. This is a different mode of cation distribution from that of Eq. (5).

The Si^{4+} partially disordered distribution in the tetrahedral and octahedral sites influences the olivine-spinel transition boundary of Fe_2SiO_4 due to an increase in the configurational entropy of spinel. Navrotsky (1977) pointed out that the cation disorder in Fe_2SiO_4 spinel would give rise to the curvature in the slope of the P–T boundary for the olivine-spinel transition.

Discussion

The spinel structure has four tetrahedral cations (M_T) and eight octahedral cations (M_O) in the unit cell. The magnetic moment is due to a super exchange between magnetic ions in both sites. Interatomic distances be-

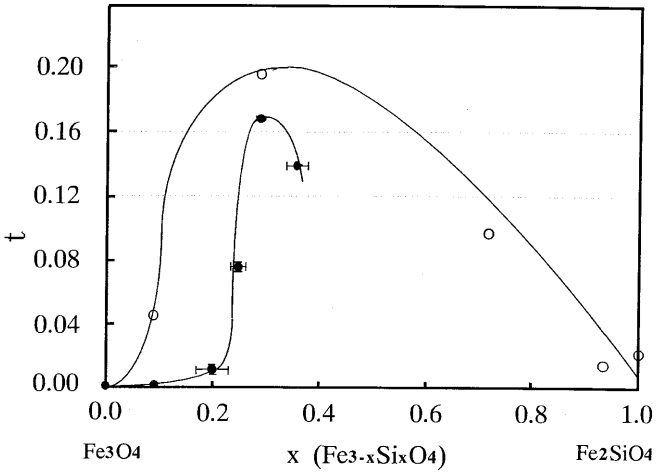

Fig. 5 Ordering parameter t in $^{\text{tetr}}[Fe^{3+}_{1-x+xt}Si^{4+}_{x(1-t)}]^{\text{octa}}$ $[Fe^{2+}_{1+x}Fe^{3+}_{1-x-xt}Si^{4+}_{xt}]O_4$. Site occupancies were determined by X-ray diffraction analysis (*open circle*) and saturation magentization (*closed circle*)

Table 4 Cation distribution of $Fe_{3-x}Si_xO_4$ spinel solid solutions

x $Fe_{3-x}Si_xO_4$	Saturation magnetization (μ_B)	Tetrahedral site		Octahedral site			t
		Fe^{3+}	Si^{4+}	Fe^{2+}	Fe^{3+}	Si^{4+}	
		Site occupancy estimated from magnetic moment					
0.00	4.18	1.00	0.00	1.00	1.00	0.00	
0.090	4.35	0.989	0.081	1.090	0.909	0.001	0.001
0.199	4.69	0.803	0.197	1.199	0.799	0.002	0.011
0.226	4.76	0.790	0.210	1.226	0.758	0.016	0.072
0.288	4.67	0.760	0.240	1.288	0.664	0.048	0.167
0.357	4.92	0.694	0.306	1.357	0.592	0.051	0.142
0.794	3.45						
		Site occupancy from X-ray diffraction study					
0.000	–	1.000	0.000	1.000	1.000	0.000	0.000
0.090	–	0.914	0.086	1.090	0.906	0.004	0.044
0.288	–	0.769	0.231	1.288	0.662	0.057	0.198
0.750	–	0.324	0.676	1.750	0.176	0.074	0.099
1.000	–	0.024[a]	0.976	1.976	0.000	0.024	0.024

$^{\text{tetr}}[Fe^{3+}_{1-x+xt}Si^{4+}_{x(1-t)}]^{\text{octa}}[Fe^{2+}_{1+x}Fe^{3+}_{1-x-xt}Si^{4+}_{xt}]O_4$

[a] Site occupancy of ferrous ion instead of ferric ion

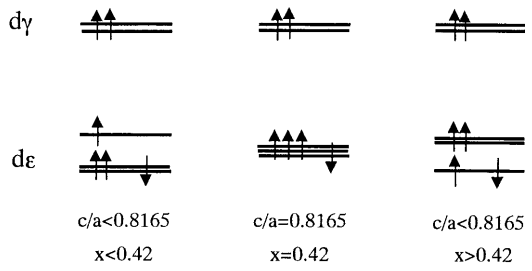

Fig. 6 Electron configuration change by crystal field

tween the two cations are defined by the lattice constant. The M_O cation has six nearest M_O cations in a distance of about 2.97 Å and six second-neighbor M_T with about 3.48 Å, which is obtained from X-ray diffraction study (Yamanaka et al. 1998). On the other hand, M_T has 12 nearest M_O in a distance of about 3.48 Å and 4 second-neighbor M_T in 3.63 Å. $Fe_{3-x}Si_xO_4$ cation distribution reflects the probability of the super exchange. M_O and M_T have antiparallel spin. If M_s is produced only by the magnetic spin moment and all M_T is $Fe^{3+}(x = 0.0)$, $M_B = \{5\mu_B \times 6(Fe_O^{3+}) + 4\mu_B \times 6(Fe_O^{2+}) - 5\mu_B \times 6(Fe_T^{3+}) \times (2.967/3.491)\}/6 = 4.750\mu_B$ according to Eq. (2). When 1/6 of M_T is $Si^{4+}(x = 0.1667)$, $M_B = \{5\mu_B \times 5(Fe_O^{3+}) + 4\mu_B \times 7 \quad (Fe_O^{2+}) - 5\mu_B \times 5(Fe_T^{3+}) \quad (2.965/3.4485\}/6 = 5.2508\mu_B$.

The Curie temperature T_c is decreased with increasing nonmagnetic Si^{4+} ion in the $Fe_{3-x}Si_xO_4$ spinel structure. The Fe–Fe interaction J_{AB} in Eq. (4) of $Fe_{3-x}Si_xO_4$ is the dominant constraint to the temperature. The magnetic moment is indeed controlled by the concentration of Fe^{2+} and Fe^{3+} in the tetrahedral and octahedral sites. In general, when the cation distance is shorter and the M_T-O-M_O angle approaches nearer to 180°, the super exchange interaction between magnetic cations becomes larger. According to X-ray structure analysis (Yamanaka et al. 1998), the angle changes from 123.7° ($x = 0.0$) to 128.7° ($x = 1.0$), and the cation distances M_T–M_T, M_O–M_O, and M_T–M_O become shorter with increasing Fe_2SiO_4 content; but the differences in these angles and distances are not sufficient to bring about such a large difference in M_s. Thus, the site occupancies Z_{AB} of this solid solution system are likely to be the dominant effect for W_{AB} in Eq. (4).

Judging from the oxygen positional parameter (u), the crystal field at the octahedral site is changed at the boundary of $u = 0.375$. The boundary composition is estimated to be $x = 0.42$. From the electron spin configuration shown in Fig. 6, the energetically lowest level in dε in the region of $x < 0.42$ is degenerate and in those samples results in an orbital angular momentum; but in the case of $x > 0.42$, the level becomes a singlet and has no orbital angular momentum. Then, only spin momentum is taken into consideration for those samples having $x > 0.42$.

In the solid solutions having $x > 0.375$, the antiparallel mode of magnetic spins between M_T and M_O is disturbed and lowers the magnetization. The parallel spins in the octahedral site are also gradually disturbed with increasing Fe^{2+} in the site. Finally, in Fe_2SiO_4 ($x = 1.0$), the randomized spins induce a paramagnetic character at temperatures above T_N and they become antiferromagnetic below $T_N = 12$ K due to M_O–M_O interaction.

Acknowledgements We are indebted to Prof. Y. Miyako and Dr. C. Ueda in the Faculty of Science, Osaka University, for their kind help for magnetic measurement facility. The present series of works are partly supported by the Grants-in-Aid nos. A(2)-10304044 and B(2)-11694076 of the Ministry of Education, Science, Sport, and Culture, Japan.

References

Akaogi M, Akimoto S, Horioka K, Takahashi K, Horiuchi H (1982) The system $NiAl_2O_4$-Ni_2SiO_4, at high pressures and temperatures: spinelloids with spinel-related structures. J Solid State Chem 44: 257–267

Aragon R, Buttrey DJ, Shephered JP, Honig JM (1985) Influence of nonstoichiometry on the Verwey transition. Phys Rev (B)31: 430–436

Brown NE, Navrotsky A, Nord GL Jr, Banerjee SK (1993) Hematite-ilmenite (Fe_2O_3-$FeTiO_3$) solid solution: determinations of Fe–Ti order from magnetic properties. Am Mineral 78: 941–951

Canil D, O'Neill H, Ross II CR (1990) A preliminary look at phase relations in the system Fe_3O_4-γ-Fe_2SiO_4 at 7 GPa. Terra Abstr 3: 65

Darken LS, Gurry RW (1945) The system iron-oxygen I. The wüstite field and related equilibria. J Am Ceram Soc 67: 1398–1412

Fei Y, Frost DJ, Mao HK, Prewitt CT, Heuserman D (1999) In situ determination of the high-pressure phase of Fe_3O_4. Am Mineral 84: 203–206

Harrison RJ, Putnis A (1995) Magnetic properties of the magnetic-spinel solid solution: saturation magnetization and cation distributions. Am Mineral 80: 213–221

Horioka K, Takahashi K, Morimoto N, Horiuchi M, Akaogi M, Akimoto S (1981) Structure of nickel aluminosilicate (phase V): a high-pressure phase related to spinel. Acta Crystallogr (B) 37: 635–638

Irifune T, Ringwood AE (1987) Phase transformation in primitive MORB and pyrolite compositions to 25 GPa and some geophysical implications. In: Maghnani M, Syono Y (eds) High pressure research in mineral physics. Am Geophysicea Union Washington DC, pp 231–242

Kronmuller H, Walz F (1980) Magnetic after-effects in Fe_3O_4 and vacancy-doped magnetite. Philos Mag 42: 433–452

Krupicka S, Novàk P (1987) Ferromagnetic materials: A hand book on the properties of magnetically ordered substances. In: Wohlfarth EP (ed), 189–304

Ma CB (1974) New olivine phase on the join $NiAl_2O_4$ (spinel analogue)-Ni_2SiO_4 (olivine analogue): stability and implications to mantle mineralogy. Contrib Miner Petrol 45: 257–279

Mao HK, Takahashi T, Bassett WA, Kinsland GL, Merril L (1974) Isothermal compression of magnetite to 320 kbar and pressure-induced phase transformation. J Geophys Res 79: 1165–1170

Marumo F, Isobe M, Saito Y, Yagi T, Akimoto S (1974) Electron density distribution in crystals of γ-Ni_2SiO_4. Acta Crystallogr (B) 30: 1904–1906

Marumo F, Isobe M, Akimoto S (1977) Electron-density distribution in crystals of γ-Fe_2SiO_4 and γ-Co_2SiO_4. Acta Crystallogr (B) 33: 713–716

Morrish AH (1965) The physical properties of rock magnetism. Wiley, New York, 680 pp

Navrotsky A (1977) Calculation of effect of cation disorder on silicate spinel phase boundaries. Earth Plan Sci Lett 33: 437–442

Ohtaka O, Tobe H, Yamanaka T (1997) Phase equilibria for the Fe_2SiO_4-Fe_3O_4 system under high pressure. Phys Chem Miner 24: 555–560

O'Neill HStC, Canil D (1992) Phase relations along the join Fe_3O_4-Fe_2SiO_4 at 7 and 9 GPa and the oxidation state of the transition zone. In: Abstract of AGU Spring Meeting, 298

O'Neill HStC, McCammon CA, Canil D, Rubie DC, Ross II CR, Seifert F (1993) Mössbauer spectroscopy of mantle transition zone phases and determination of minimum Fe^{3+} content. Am Mineral 78: 456–460

Pasternak MP, Nasu S, Wada K, Endo S (1994) High-pressure phase of magnetite. Phys Rev (B) 50: 6446–6449

Ross II CR, Armbruster T, Canil D (1992) Crystal structure refinement of a spinelloid in the system Fe_3O_4-Fe_2SiO_4. Am Mineral 77: 507–511

Suito K, Tsutsui Y, Nasu S, Onodera A, Fujuta FE (1984) Mössbauer effect study of the γ-form Fe_2SiO_4. Mat Res Soc Symp Proc 22: 295–298, Elsevier Science Publishing Co.

Verwey EJ (1939) Electronic condition of magnetite (Fe_3O_4) and its transition point at low temperatures. Nature 144: 327–987

Woodland AB, Angel RJ (1998) Crystal structure of a new spinelloid with the wadsleyite structure in the system Fe_2SiO_4-Fe_3O_4 and implications for the Earth's mantle. Am Mineral 83: 404–408

Yamanaka T (1986) Crystal structure of Ni_2SiO_4 and Fe_2SiO_4 as a function of temperature and heating duration. Phys Chem Miner 13: 227–232

Yamanaka T, Tobe H, Shimazu H, Nakatsuka A, Dobuchi Y, Ohtaka O, Nagai T, Ito E (1998) Phase relations and physical properties of Fe_2SiO_4-Fe_3O_4 solid solution under pressures up to 12 GPa. Properties of Earth and planetary materials at high pressure and temperature. Monograph of the American Geophysical Union, Washington DC, 101: 451–459

Yamanaka T, Shimazu H, Ota K (2001) Electric conductivity of the Fe_2SiO_4-Fe_3O_4 spinel solid solutions. Phys Chem Miner 28: 110–118